Supporting Information

Highly Efficient Electrochemical Synthesis of Hydrogen Peroxide (H_2O_2) Enabled by Amino Acid Glycine-Derived Metal-Free Nitrogen-Doped Ordered Mesoporous Carbon

Basil Sabri Rawah [†], Mohammad Albloushi[†] and Wenzhen Li[†]*

† Chemical and Biological Engineering, Biorenewables Research Laboratory, Iowa State University, Ames, IA 50011, USA

* Correspondence authors.

Wenzhen Li - E-mail: wzli@iastate.edu; Tel: +1-515-294-4582

Number of Pages: 13

Number of Figures: 7

Number of Tables: 6

The electrochemical reduction of O_2 to H_2O (OH^-) requires four electrons (S1), whereas the partial reduction of O_2 to H_2O_2 (OH_2^-) involves two electrons (S2).

$$O_2 + 4H^+ + 4e^- \rightarrow 2H_2O \quad (pH < 11.6) \quad E^\circ = 1.23\ V$$
$$O_2 + 2H_2O + 4e^- \rightarrow 4OH^- \quad (pH > 11.6) \quad E^\circ = 0.40\ V \qquad (S1)$$

$$O_2 + 2H^+ + 2e^- \rightarrow H_2O_2 \quad (pH < 11.6) \quad E^\circ = 0.7\ V$$
$$O_2 + H_2O + 2e^- \rightarrow HO_2^- + OH^- \quad (pH > 11.6) \quad E^\circ = 0.06\ V \qquad (S2)$$

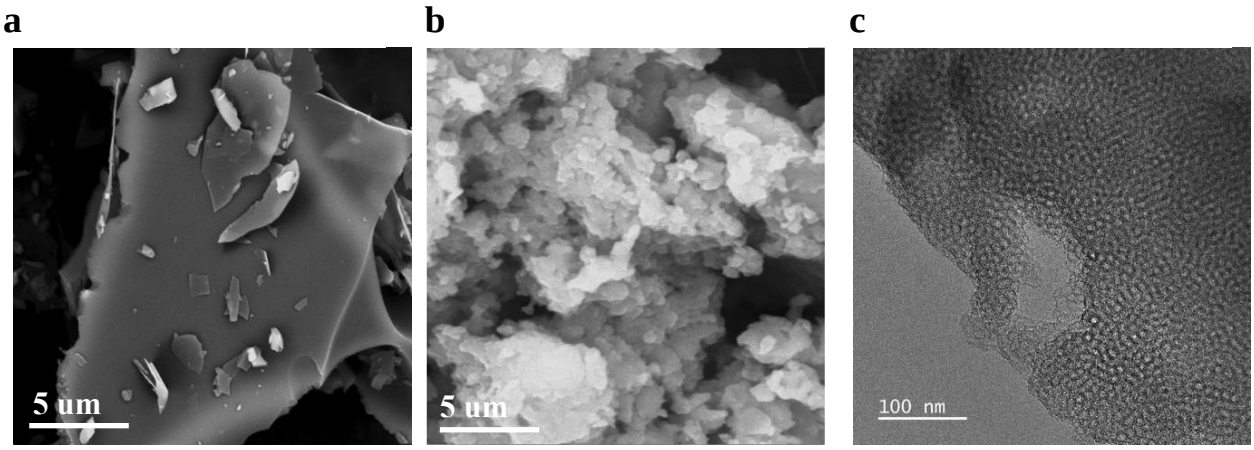

Figure S1. SEM images (a) KIT-6-free-N-C, (b) KIT-6 and TEM image (c) of KIT-6.

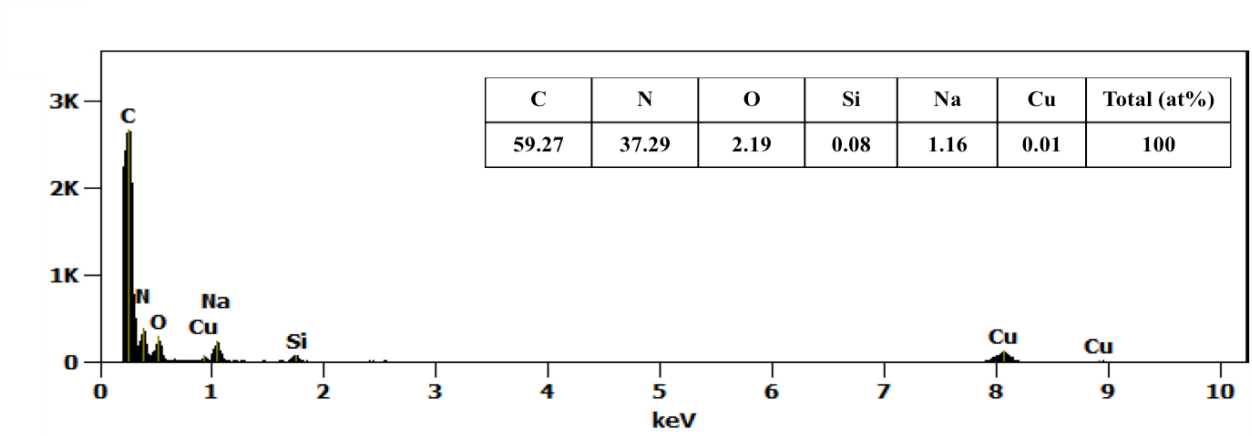

C	N	O	Si	Na	Cu	Total (at%)
59.27	37.29	2.19	0.08	1.16	0.01	100

Figure S2. EDS elemental mapping and atomic percentage of N-OMC-800. The Cu intensity is a background noise caused by the instrument.

a **b**

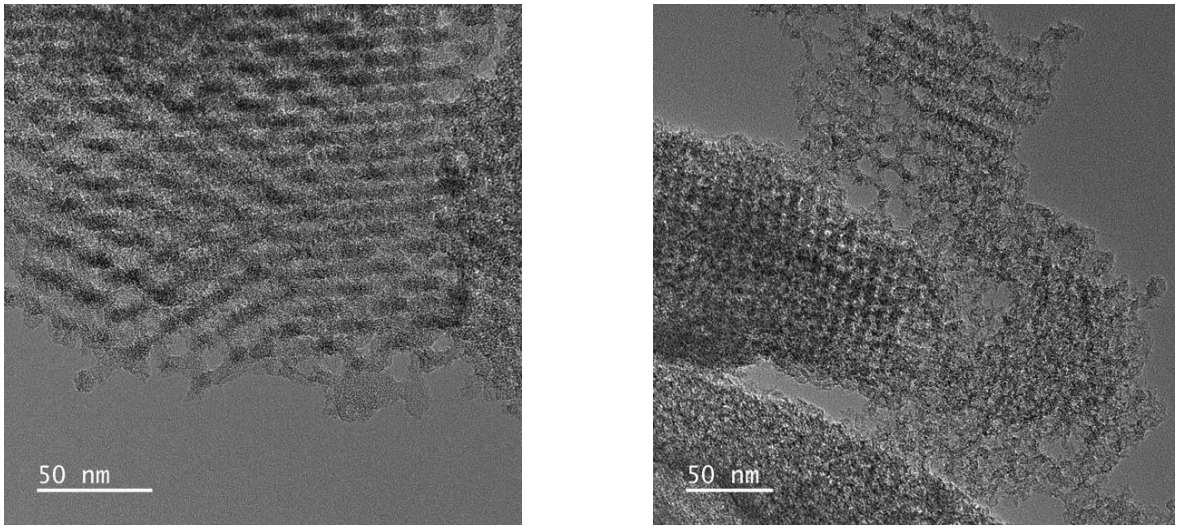

Figure S3. TEM images of (a) N-0MC-700 and (b) N-OMC-900.

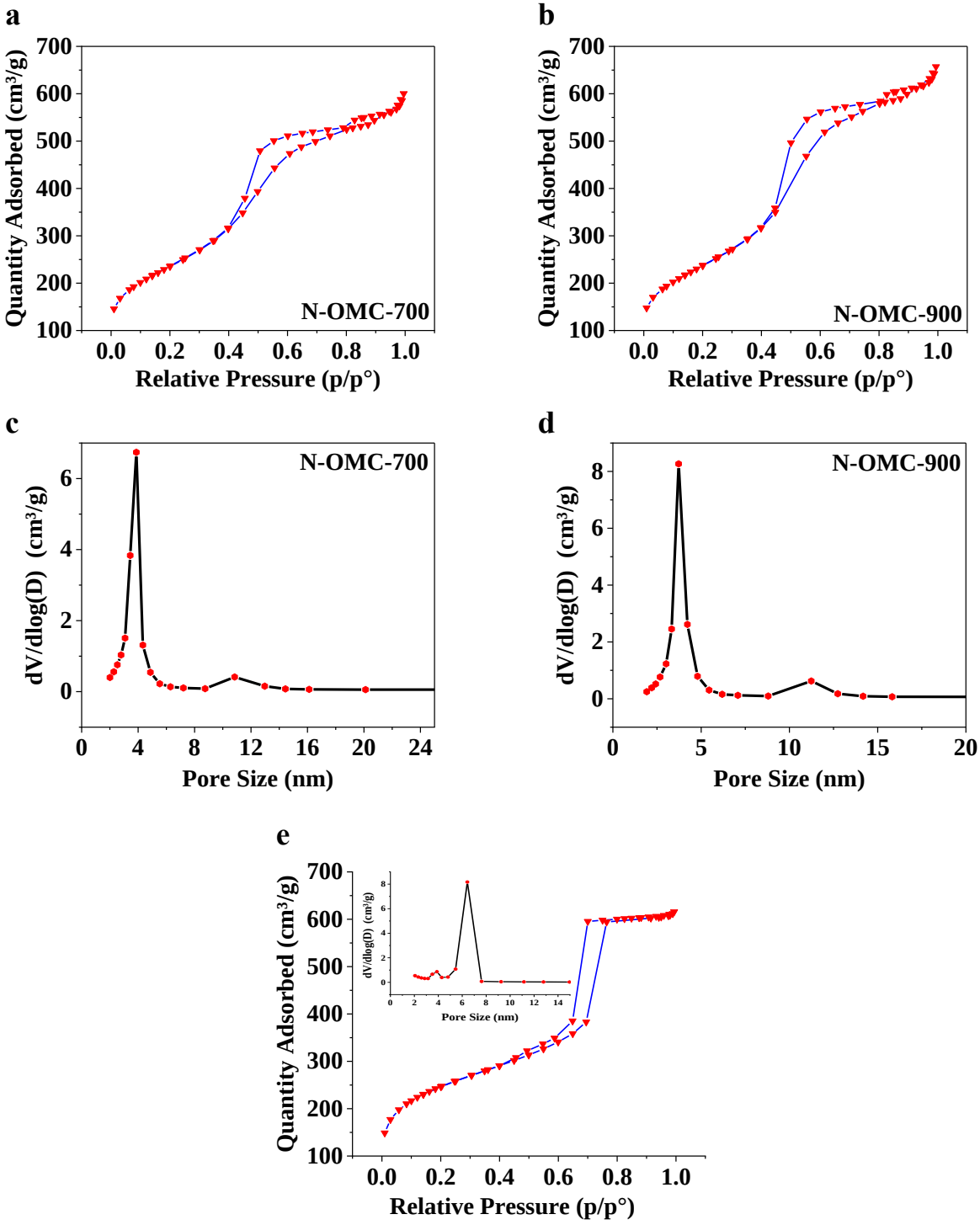

Figure S4. Nitrogen adsorption–desorption isotherms of (a) N-OMC-700, (b) N-OMC-900 and (e) KIT-6 and pore size distribution (c) N-OMC-700 and (d) N-OMC-900 and (e Inset) KIT-6.

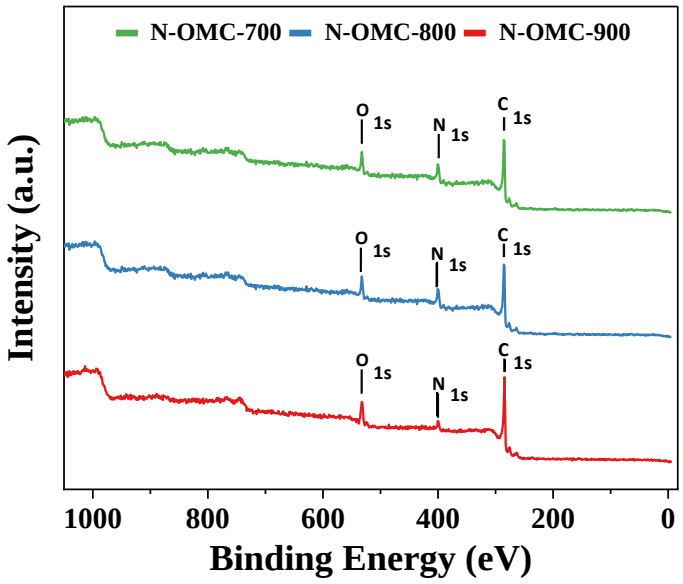

Figure S5. XPS survey spectra of all N-OMCs.

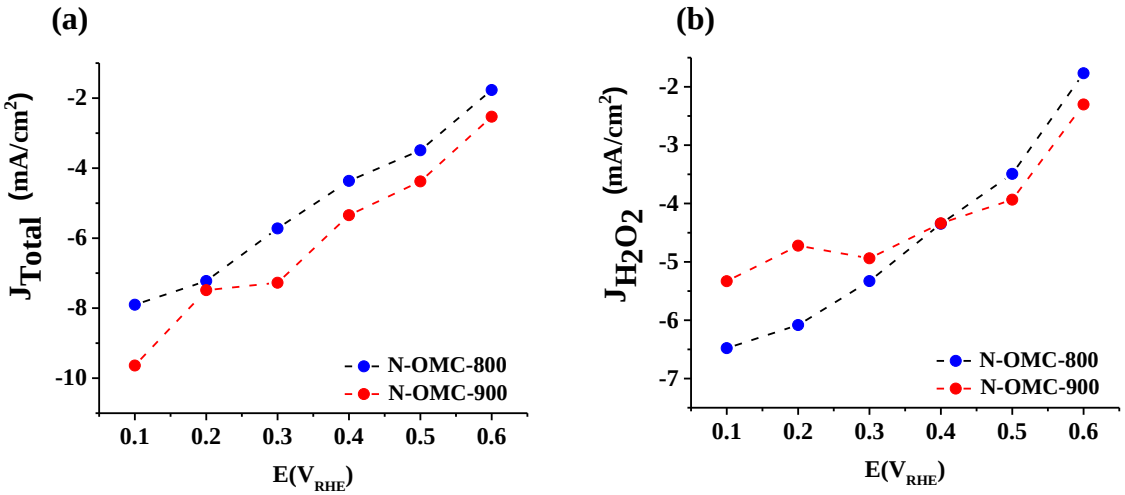

Figure S6. (a) Total current density (b) Partial current density of N-OMC-800 (blue) and N-OMC-900 (red) at varied potential range conducted in 0.1M KOH for 1h with catalyst loading of 0.1 mg/cm^2.

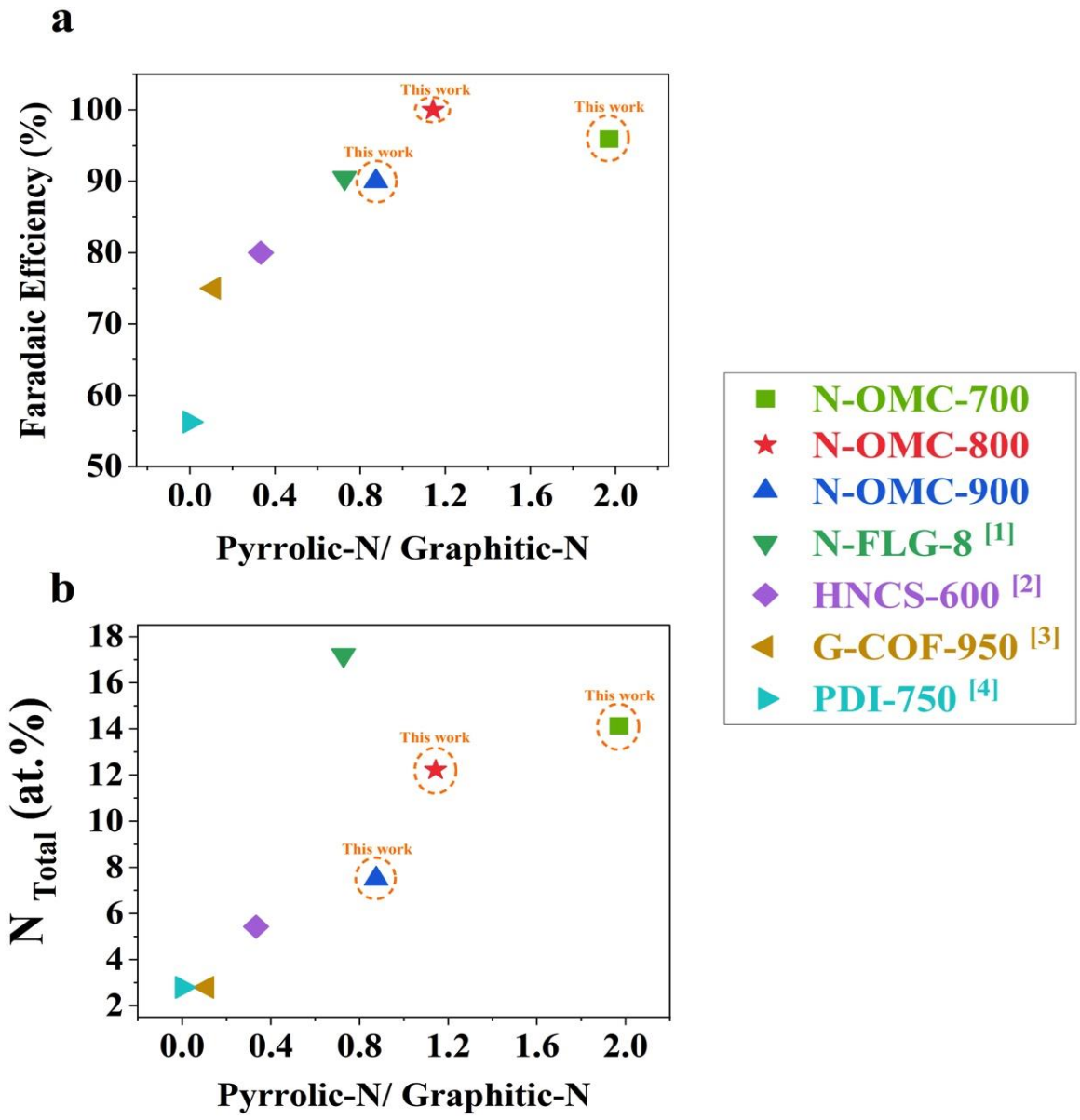

Figure S7. P/G atomic ratio vs. (a) H_2O_2 faradaic efficiency (%) and (b) vs. N-total (at.%) of N-OMCs and state of art nitrogen doped carbon $2e^-$ ORR catalysts in 0.1 M KOH at 0.5 V_{RHE} [1-4].

Figure S7 was adapted from the literature to provide more insight into the atomic ratio of P/G ratio. The P/G ratios of several nitrogen-doped carbons were determined, and the overall pattern indicates that as the P/G ratio decreased (< 0.8), the H_2O_2 FE (%) decreased as well. This

correlation supports the findings of this study. As with the N-OMC-800, a higher P/G ratio (near to 1) is desirable to obtain high selectivity and yield. It's worth noting that we were unable to plot P/G vs. current density since the loading was varied in each study and the disclosed data was insufficient to plot P/G vs. J.

Table S1 N_2 Adsorption analysis of all N-OMC catalysts and KIT-6 template.

Sample	BET surface Area (m^2/g)	Total Pore Volume (cm^3/g)	Micropore volume (cm^3/g)	Mesopore volume (cm^3/g)	Pore Diameter (nm)
KIT-6	877	0.94	0.094	0.861	5.54
N-OMC-700	844	0.88	0.031	0.996	4.28
N-OMC-800	864	1.08	0.033	1.23	5.12
N-OMC-900	850	0.96	0.026	1.074	4.38

Table S2 XPS elemental analysis of all N-OMCs and N-no/OMC-800 and their nitrogen to carbon ratios.

Sample	C (at.%)	N (at.%)	O (at.%)	N/C
N-OMC-700	76.77	14.13	9.09	0.18
N-OMC-800	79.63	12.22	8.15	0.15
N-OMC-900	81.42	7.51	11.08	0.09
N-no/OMC-800	85.17	8.45	6.38	0.1

Table S3 Nitrogen species atomic content of all N-OMC all N-OMCs and N-no/OMC-800 via XPS.

Sample	Pyrrolic-N (at.%)	Graphitic-N (at.%)	Pyridinic-N (at.%)
N-OMC-700	6.74	3.42	2.22
N-OMC-800	4.40	3.85	2.12
N-OMC-900	2.49	2.84	0.87
N-no/OMC-800	2.40	2.95	1.81

Table S4 Comparison of H_2O_2 Faradaic Efficiency in H-cell of N-OMC-800 with recently reported electrocatalysts in alkaline medium in H-cell/RRDE.

Sample	pH	Electrolyte	V_{RHE}	FE (%)	Reference
N-OMC-800	13	0.1 M KOH	0.6 – 0.4	~ 100	This work
Nitrogen doped mesoporous carbon	13	0.1 M KOH	0.3	70	[5]
G-COF-950, nitrogen-Doped carbon	13	0.1 M KOH	0.1	75	[3]
Co-N-C	13	0.1 M KOH	0.5	~ 55	[6]
N-FLG-8	13	0.1 M KOH	0.6	> 90.5 **(RRDE)**	[1]
Hollow N-Doped Carbon Nanospheres	13	0.1 M KOH	0.5	80.0 **(RRDE)**	[2]
CN_x800 N-Doped carbon nanotubes	13	0.1 M KOH	0.4	84.9 **(RRDE)**	[7]
Nitrogen doped Vulcan	13	0.1 M KOH	0.6	83 **(RRDE)**	[8]
NOMC-H	13	0.1 M KOH	0.6	73.5 **(RRDE)**	[9]

Table S5 Comparison of H_2O_2 bulk production in flow cell of N-OMC-800 with recently reported electrocatalysts in alkaline medium.

Catalyst	Cell Type	Potential /cell voltage	Electrolyte	Concentration ($mol/g_{cat}^{-1}h^{-1}$)	FE (%)	Reference
N-OMC-800	Flow cell	0.35 V_{RHE}	0.1M KOH	9.43	~ 100	This work
N-FLG-8	Flow cell	1.8 V	1 M KOH	9.66	99.6	[1]
Co-N-C	Flow cell	~ 2 V	0.1M KOH	4.33	~ 40	[6]
CMK3-20s	Flow cell	1.8 V	0.1 M KOH	1.28	91	[10]
CMK3-20s	Flow cell	2.4 V	0.1 M KOH	1.8	95	[10]
N-O-P-C-800	Flow cell	1.3 V	0.1 M KOH	0.54	93.1	[11]
N-O-P-C-800	Flow cell	2.5 V	0.1 M KOH	0.8	94	[11]
Ni-N2O2/C7	Flow cell	~ 0.4 V_{RHE}	0.1 M KOH	5.9	91	[12]
N-doped mesoporous carbon	H-cell	0.3 V_{RHE}	0.1 M KOH	0.5617	~ 70	[5]
G-COF-950	H-cell	0.1 V_{RHE}	0.1 M KOH	1.2869	69.8	[3]

Table S6 Comparison of the N-OMC-800 stability with state-of-the-art catalysts of H_2O_2 generation in alkaline medium.

Sample	Electrolyte	V_{RHE}	Faradaic Efficiency (%)	Stability (hours)	Reference
N-OMC-800	0.1 KOH	0.6	99.28%	12	This work
Ni-N_2O_2/C	0.1 KOH	0.5	91.1 %	8	[12]
B-C	1M KOH	0.685	85.10%	200	[8]
Co-N-C	0.1 KOH	~0.55	Not mentioned (H-cell)	110	[13]
B,N doped carbon	0.1 KOH	0.55	85.00% (RRDE)	50	[14]
O-CNT	0.1 M KOH	0.68	~ 90% (RRDE)	10	[15]
N-doped mesoporous carbon	0.1 KOH	0.3	82.00% (RRDE)	6	[5]
N-doped carbon nanohorns	0.1M NaOH	0.65	< 65% (RRDE)	25	[16]
Fe-O-CNT	0.1 M KOH	0.71	> ~ 90 (RRDE)	8	[17]

REFERENCES

1. Li, L.; Tang, C.; Zheng, Y.; Xia, B.; Zhou, X.; Xu, H.; Qiao, S. Z. Tailoring selectivity of electrochemical hydrogen peroxide generation by tunable pyrrolic-nitrogen-carbon. *Adv. Energy Mater.* **2020,** *10* (21), 2000789, DOI 10.1002/aenm.202000789.

2. Hu, Y.; Zhang, J.; Shen, T.; Li, Z.; Chen, K.; Lu, Y.; Zhang, J.; Wang, D. Efficient Electrochemical Production of H2O2 on Hollow N-Doped Carbon Nanospheres with Abundant Micropores. *ACS Appl. Mater. Interfaces* **2021**, DOI 10.1021/acsami.1c05353.

3. Zhang, J.; Zhang, G.; Jin, S.; Zhou, Y.; Ji, Q.; Lan, H.; Liu, H.; Qu, J. Graphitic N in nitrogen-doped carbon promotes hydrogen peroxide synthesis from electrocatalytic oxygen reduction. *Carbon* **2020,** *163*, 154-161, DOI 10.1016/j.carbon.2020.02.084.

4. Liu, R.; Wu, D.; Feng, X.; Müllen, K. Nitrogen-doped ordered mesoporous graphitic arrays with high electrocatalytic activity for oxygen reduction. *Angew. Chem* **2010,** *122* (14), 2619-2623, DOI 10.1002/anie.200907289.

5. Sun, Y.; Sinev, I.; Ju, W.; Bergmann, A.; Dresp, S. r.; Kühl, S.; Spöri, C.; Schmies, H.; Wang, H.; Bernsmeier, D. Efficient electrochemical hydrogen peroxide production from molecular oxygen on nitrogen-doped mesoporous carbon catalysts. *ACS Catal.* **2018,** *8* (4), 2844-2856, DOI 10.1021/acscatal.7b03464.

6. Sun, Y.; Silvioli, L.; Sahraie, N. R.; Ju, W.; Li, J.; Zitolo, A.; Li, S.; Bagger, A.; Arnarson, L.; Wang, X. Activity–selectivity trends in the electrochemical production of hydrogen peroxide over single-site metal–nitrogen–carbon catalysts. *J. Am. Chem. Soc.* **2019,** *141* (31), 12372-12381, DOI 10.1021/jacs.9b05576.

7. Contreras, E.; Dominguez, D.; Tiznado, H.; Guerrero-Sanchez, J.; Takeuchi, N.; Alonso-Nunez, G.; Contreras, O. E.; Oropeza-Guzmán, M. T.; Romo-Herrera, J. M. N-Doped carbon nanotubes enriched with graphitic nitrogen in a buckypaper configuration as efficient 3D electrodes for oxygen reduction to H 2 O 2. *Nanoscale* **2019,** *11* (6), 2829-2839, DOI 10.1039/C8NR08384C.

8. Xia, Y.; Zhao, X.; Xia, C.; Wu, Z.-Y.; Zhu, P.; Kim, J. Y. T.; Bai, X.; Gao, G.; Hu, Y.; Zhong, J. Highly active and selective oxygen reduction to H2O2 on boron-doped carbon for high production rates. *Nat. Commun.* **2021,** *12* (1), 1-12, DOI 10.1038/s41467-021-24329-9.

9. Sheng, X.; Daems, N.; Geboes, B.; Kurttepeli, M.; Bals, S.; Breugelmans, T.; Hubin, A.; Vankelecom, I. F. J.; Pescarmona, P. P. N-doped ordered mesoporous carbons prepared by a two-step nanocasting strategy as highly active and selective electrocatalysts for the reduction of O2 to H2O2. *Appl. Catal. B* **2015,** *176*, 212-224, DOI 10.1016/j.apcatb.2015.03.049.

10. Wang, Y.-L.; Li, S.-S.; Yang, X.-H.; Xu, G.-Y.; Zhu, Z.-C.; Chen, P.; Li, S.-Q. One minute from pristine carbon to an electrocatalyst for hydrogen peroxide production. *J. Mater. Chem. A* **2019,** *7* (37), 21329-21337, DOI 10.1039/c9ta04788c.

11. Zhang, H.-X.; Yang, S.-C.; Wang, Y.-L.; Xi, J.-C.; Huang, J.-C.; Li, J.-F.; Chen, P.; Jia, R. Electrocatalyst derived from fungal hyphae and its excellent activity for electrochemical production of hydrogen peroxide. *Electrochim. Acta* **2019,** *308*, 74-82, DOI 10.1016/j.electacta.2019.04.011.

12. Wang, Y.; Shi, R.; Shang, L.; Waterhouse, G. I. N.; Zhao, J.; Zhang, Q.; Gu, L.; Zhang, T. High-Efficiency Oxygen Reduction to Hydrogen Peroxide Catalyzed by Nickel Single-Atom

Catalysts with Tetradentate N2O2 Coordination in a Three-Phase Flow Cell. *Angew. Chem. Int. Ed.* **2020,** *59* (31), 13057-13062, DOI 10.1002/anie.202004841.

13. Jung, E.; Shin, H.; Lee, B.-H.; Efremov, V.; Lee, S.; Lee, H. S.; Kim, J.; Antink, W. H.; Park, S.; Lee, K.-S. Atomic-level tuning of Co–N–C catalyst for high-performance electrochemical H 2 O 2 production. *Nat. Mater* **2020,** *19* (4), 436-442, DOI 10.1038/s41563-019-0571-5.

14. Chen, S.; Chen, Z.; Siahrostami, S.; Higgins, D.; Nordlund, D.; Sokaras, D.; Kim, T. R.; Liu, Y.; Yan, X.; Nilsson, E. Designing boron nitride islands in carbon materials for efficient electrochemical synthesis of hydrogen peroxide. *J. Am. Chem. Soc.* **2018,** *140* (25), 7851-7859, DOI 10.1021/jacs.8b02798.

15. Lu, Z.; Chen, G.; Siahrostami, S.; Chen, Z.; Liu, K.; Xie, J.; Liao, L.; Wu, T.; Lin, D.; Liu, Y. High-efficiency oxygen reduction to hydrogen peroxide catalysed by oxidized carbon materials. *Nat. Catal.* **2018,** *1* (2), 156-162, DOI 10.1038/s41929-017-0017-x.

16. Iglesias, D.; Giuliani, A.; Melchionna, M.; Marchesan, S.; Criado, A.; Nasi, L.; Bevilacqua, M.; Tavagnacco, C.; Vizza, F.; Prato, M. N-doped graphitized carbon nanohorns as a forefront electrocatalyst in highly selective O2 reduction to H2O2. *Chem* **2018,** *4* (1), 106-123, DOI 10.1016/j.chempr.2017.10.013.

17. Jiang, K.; Back, S.; Akey, A. J.; Xia, C.; Hu, Y.; Liang, W.; Schaak, D.; Stavitski, E.; Nørskov, J. K.; Siahrostami, S. Highly selective oxygen reduction to hydrogen peroxide on transition metal single atom coordination. *Nat. Commun.* **2019,** *10* (1), 1-11, DOI 10.1038/s41467-019-11992-2.